

LRP 363/88

November 1988

DEFLECTION TYPE ENERGY ANALYSER FOR  
ENERGETIC ELECTRON BEAMS IN A  
BEAM-PLASMA SYSTEM

J.-A. Michel and J.-P. Hogge

*to be published in*  
*Review of Scientific Instruments*

**Deflection type energy analyser for energetic electron beams in a beam-plasma system**

J.-A. Michel and J.-P. Hogge

Centre de Recherche en Physique des Plasmas

Association Euratom - Confédération Suisse

Ecole Polytechnique Fédérale de Lausanne

21, Av. des Bains, CH-1007 Lausanne/Switzerland

**Abstract**

An energy analyser for the study of electron beam distribution functions in unmagnetized plasmas is described. This analyser is designed to avoid large electric fields which are created in multi-grid analysers and to measure directly the beam distribution function without differentiation. As an example of an application we present results on the propagation of an energetic beam ( $E_b : 2.0 \text{ KeV}$ ) in a plasma ( $n_0 : 1 \cdot 10^{10} \text{ cm}^{-3}$ ,  $T_e : 1.4 \text{ eV}$ ).

## 1. Introduction

The nonlinear interaction of an electron beam with a plasma is a very interesting phenomenon studied these last years both experimentally and theoretically.<sup>1-6</sup> In the case of strong Langmuir turbulence,<sup>5</sup> the theory predicts the propagation of the beam over large distances and the excitation of Langmuir turbulence along the beam path. The evolution of electrostatic waves is governed by the modulational instability of density fluctuations.<sup>6</sup> The relationship between the development of the modulational instability and density cavities has been carefully studied.<sup>3</sup> Less attention has been paid to the propagation of the beam itself in the case of strong turbulence. Our experiment is dedicated to the study of the thermalization distance of an energetic electron beam travelling through a steady state plasma under conditions of strong turbulence.

The main experimental difficulty encountered in earlier studies has been the determination of the beam distribution function. In standard multi-grid analysers, electrons are discriminated in kinetic energy by a retarding potential.<sup>7</sup> The collected current is an integral over electrons having enough velocity to overcome the potential barrier. The distribution function is the derivative of the current with respect to the applied potential. This operation performed on noisy signals can be problematic. A second difficulty is the problem of arcing inside the analyser structure. The distances between the grids of such analysers are generally fixed by two contradictory requirements: the energy resolution is improved by increasing the grids spacing<sup>9</sup> while, in contrast, space charge effects are minimized by decreasing their separation.<sup>8,9</sup> Typically the desired energy resolution is 6% and the current density corresponding to our experimental conditions is  $0.5 \text{ A/cm}^2$ . These requirements yield (taking a safety

factor of 10 for the current density) an optimum spacing of approximately 1.5 mm. Unfortunately, arcing problems have arisen when we have employed the standard multigrid analyser to diagnostic energetic beams above 1.3 KeV.

In order to overcome the restrictive operating conditions of previous designs, we have developed an analyser based on the principle of electron deflection by an electric field. Instead of slowing down the electrons by a high electric field parallel to the electron trajectories as in a standard multi-grid analyser, we used a lower perpendicular electric field to deflect the electrons, thus having the benefits of lower voltages and a larger gap between the biased plates (the plasma density is negligible inside this type of analyser). The analyser entry consists of a slot selecting a sheet of the beam electrons. The slot also performs the function of angular discrimination of electron trajectories. Having passed this aperture, the electrons are deflected by a DC perpendicular electric field produced by two polarized plates. Finally, a thin plate collects a selective class of electrons with energies fixed by the analyser geometry. The distribution function is obtained by multiplying the current-voltage characteristic of the analyser by a simple scaling function.

## 2. Design and Sensitivity of the Analyser

The analyser structure is shown in Fig.1. If we assume that the potential due to space charge is negligible, the electron motion is determined by the applied electric field and the initial velocity. Let us compute the required potential  $V_s$  that would deflect to the center of the collector C an electron which enters the analyser with a velocity  $V_0$  and with an entrance angle  $\alpha$ . The transit time inside the analyser is given by:

$$T_t = \frac{L}{V_o \cos\alpha} \quad (1)$$

Here L represents the distance between the analyser entry and the collector C.

The applied potential  $V_s$  between the plates of spacing D produces a perpendicular electric field  $V_s/D$ . During the transit time the collected electron has to travel the height of the analyser entry H so that:

$$H = -\frac{1}{2} \frac{e}{m} \frac{V_s}{D} T_t^2 + V_o T_t \sin\alpha \quad (2)$$

where e and m are the electron charge and mass.

Equation (2) is solved to determine the value of the deflecting potential which leads to a collected signal in the case of a monokinetic electron beam with a uniform angular distribution over the analyser acceptance angle  $\alpha$ .

Solving (2) for  $\alpha \ll 1$  we get the required potential:

$$V_s = \frac{4HD E_o}{L^2} \cdot (1 - L\alpha/H) \quad (3)$$

This condition may be expressed for the analyser as the product of a dispersive term and a "gain" between the voltage applied to the deflective plates and the energy of the measured electrons  $E_o$  (in eV).

Because of the requirement for adequate energy resolution, the quantity  $(1 - \alpha L/H)$  is close to 1. Equation (3) shows that a electron having an energy  $E_o$  could be deflected to the collector C using a low voltage,  $V_s \approx E_o / (L^2/4HD)$ . To compute the resolution of the analyser, we assume that the incoming electrons are monoenergetic.

Using (3), and taking into account the finite size of the input slots and of the collector, the worst case resolution is given by:

$$\frac{\Delta V_s}{V_s} = \frac{L}{H} \alpha + 2 \frac{\Delta L}{L} + \frac{\Delta H}{H} \quad (4)$$

$\Delta L$  and  $\Delta H$  are the width of the collector and the height of entry slot.

For beams with a finite temperature, equation 4 indicates that for a given deflecting potential  $V_s$ , the detected part of the electron distribution function will be within  $E_0(1-\Delta V_s/V_s)$  and  $E_0(1+\Delta V_s/V_s)$ . The collected current is to first order :

$$I_c \propto \int_{v_1}^{v_2} F(v) v dv \propto \int_{E_0(1-\frac{\Delta V_s}{V_s})}^{E_0(1+\frac{\Delta V_s}{V_s})} F(E) dE \cong F(E)|_{E=E_0} * 2 \frac{\Delta V_s}{V_s} E_0 \quad (5)$$

Equation (5) shows that the current is directly proportional to the distribution function  $F(E)$  and the sensitivity ( $2E_0 \Delta V_s/V_s$ ). Accordingly, at low energy the sensitivity is low. However, the fact that  $F(E)$  is obtained directly from  $I_c$  allows us to use this analyser in an energy domain where the collected current  $I_c$  is small and often noisy.

An analyser was constructed with the following parameters :

Deviation length :	$L = 60$ mm
Distance between the deflecting plates :	$D = 20$ mm
Acceptance angle (slot of 1mm over 40mm):	$\alpha = 0.025$ rad.
Height of the slot :	$H = 19.5$ mm
Size of the collector :	$\Delta L = 1.5$ mm

With the geometrical parameters given above, it has a gain =  $E_0/V_S$  of 2.3eV/V and a dispersion  $\Delta V_S/V_S$  of 17.9%. The dispersion value given here is obtained by using first order estimations. The exact characteristic of the analyser was calculated by integration of the electron trajectories. Figure 2 shows the current produced by a monoenergetic electron beam with a uniform angular distribution over the analyser acceptance angle. Of particular importance is the I-V characteristic of the analyser for a given gaussian distribution function of the incident electrons. In order to demonstrate the effect of the instrumental bandwidth on the measured distribution, we have plotted (Fig. 3) the full width at half maximum (FWHM) of the characteristic as a function of the FWHM of the distribution function.

It is important to note that the two FWHM agree for distribution functions having an energy spread larger than about 18%. The influence of the instrumental broadening on the amplitude of the signal  $I_C$  (cf. Eq. 5) is already negligible when the FWHM of the input distribution function exceeds 16.5%.

### 3. Experimental test of the analyser

An analyser of the afore-mentioned design was applied to measure electron distribution functions in a beam-plasma system with the following parameters<sup>10</sup>:  
 $n_0$ :  $0.5 \cdot 10^{10} \text{ cm}^{-3}$ ,  $T_e$ : 0.7 eV,  $n_b/n_0$ : 1.5 %,  $E_b$ : 2.0 KeV,  $V_b/V_{te} = 53.5$ ,  $K_b$ :  $2.1 \text{ cm}^{-1}$ , beam pulse length: 5 - 30  $\mu\text{s}$ .  $V_b$ ,  $V_{te}$ ,  $K_b$  are respectively the beam velocity, the electron thermal velocity  $(2T_e/m_e)^{1/2}$ , and the wavenumber of the resonant wave ( $\omega_{pe}/V_b$ ). Since the cathode is directly heated, there is a voltage drop of about 30 V across it. The energy spread of the beam is therefore at least 30 eV.

Theory<sup>5</sup> predicts that the normalized beam energy ( $E_b/T_e$ ) and density ( $n_b/n_0$ ) in our experiment correspond to strong Langmuir turbulence regime. The enhanced level of Langmuir waves leads to the production of density cavitons in which the waves are trapped. As a result the beam is decoupled from the plasma waves and is able to travel large distances without being thermalized.

In our pulsed experiment the typical resolution time scale must be of the order of 0.5  $\mu$ s. The good reproducibility of the beam pulse from one discharge to another permits us to fix the deflecting potential to measure one energy class of electrons, and to reconstruct the full distribution by varying the potential from one series of pulses to another. The data are digitized and the distribution is reconstructed, taking into account the analyser sensitivity. Langmuir waves are detected by small antennae connected through a coupling capacitor to the RF detection system.

As soon as the beam was injected, Langmuir waves appeared in the vicinity of the cathode<sup>10</sup>. At later times we measured a displacement of the electrostatic waves away from the cathode (Fig. 4). Before the end of the injection the extent of this quiet region decreased. The beam energy and dispersion changed only slightly up to the end of the region where Langmuir waves appeared (Figs. 5-7). Further away the beam was thermalized quickly. The observed temperature of the beam was large compared to the instrumental broadening, allowing immediate interpretation of the analyser I-V characteristic with negligible corrections.

These results show the appearance of a quiet region between the cathode and interaction region. Theory does not predict such a non-interacting zone. Perhaps this region may be explained by the presence of a high level of low frequency plasma



fluctuations which stops the coupling between the waves and the beam. One of our future goals is to study carefully the different parameters of the plasma in this zone and the eventual relaxation of the quiet region for long duration beams.

#### 4 ) Conclusions

We have developed a new type of energy analyser for energetic electron beams injected into low density plasmas. Its sensitivity is  $E_0$  with a "gain" between the applied voltage and the analysed electron energy of 2.3 eV/V. The minimum beam temperature measurable without taking into account a dispersion due to the analyser is 16.5% of the beam energy. The signal given by the analyser is directly related to the beam distribution function and allows us to measure beams in noisy environments, where multi-grid analysers cannot be used because of the requirement of a derivative versus the applied potential. With the possibility to detect distribution functions up to 5 KeV, this new analyser allows us to study more carefully than previously the beam plasma interaction.

This work was partially supported by the Swiss National Science Foundation under grants 2.868-0.85 and 2.869-0.85. We would like to thank Dr. T. Good for helpful discussions.

References

- 1 S.V.ANTIPOV et al., Physica 3D 1-2, 311 (1981).
- 2 R.W.BOSWELL et al., Physics Letters 101A, 9, 501 (1984).
- 3 P.Y.CHEUNG and A.Y.WONG, Phys. Review Letters 55, 1880 (1985).
- 4 N.V. ASTRAKHANTSEV et al., Physics Letters 110A, 3, 129 (1985).
- 5 A.A.GALEEV et al., Sov. Phys. JETP 45(2), 266 (1977).
- 6 M.V.GOLDMAN, Rev. of Modern Physics 56(4), 709 (1984).
- 7 R.L.STENZEL et al., Rev. Sci. Instrum. 54(10), 1302 (1983).
- 8 S. STEPHANAKIS, Rev. Sci. Instrum. 39(11), 1714 (1968).
- 9 R. JONES, Rev. Sci. Instrum. 49(1), 21 (1978).
- 10 J.-A.MICHEL et al., Proc. Contr. Papers of 1987 Int. Conf. on Plasma Physics, Kiev, USSR, 1987, Vol. 3, p. 242 (1987).

### Figure Captions

**Fig. 1:** Structure of the deflection analyser.

- A: slot with an angular discrimination  $\alpha$  and a height H relative to the collector
- B: polarized plates with spacing D
- C: collector with a position L relative to the beginning of the deflection

**Fig. 2:** Collected current versus the applied voltage on the plate B. The simulation was performed for a monoenergetic beam of 1keV.

**Fig. 3:** Theoretical broadening of the detected distribution function due to the analyser.

**Fig. 4:** Longitudinal profile of the electrostatic wave intensity for different times after beam injection, with  $n_b/n_0 = 1.5 \%$ ,  $V_b/V_{te} = 53.5$ .

**Fig. 5:** Beam distribution function after 3  $\mu$ S.

**Fig. 6:** Spatial dependence of the beam energy ( $t = 3 \mu$ S).

**Fig. 7:** Spatial dependence of the beam width ( $t = 3 \mu$ S)

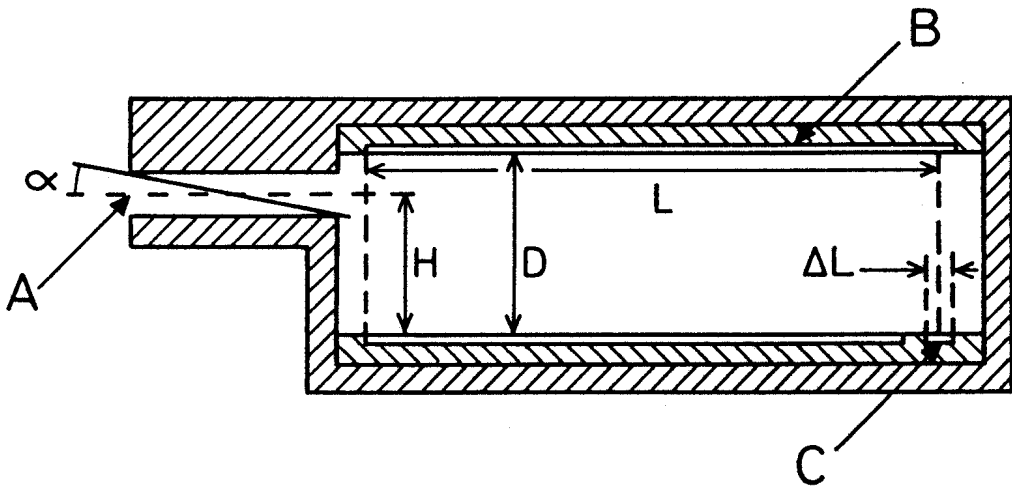


FIG. 1

---

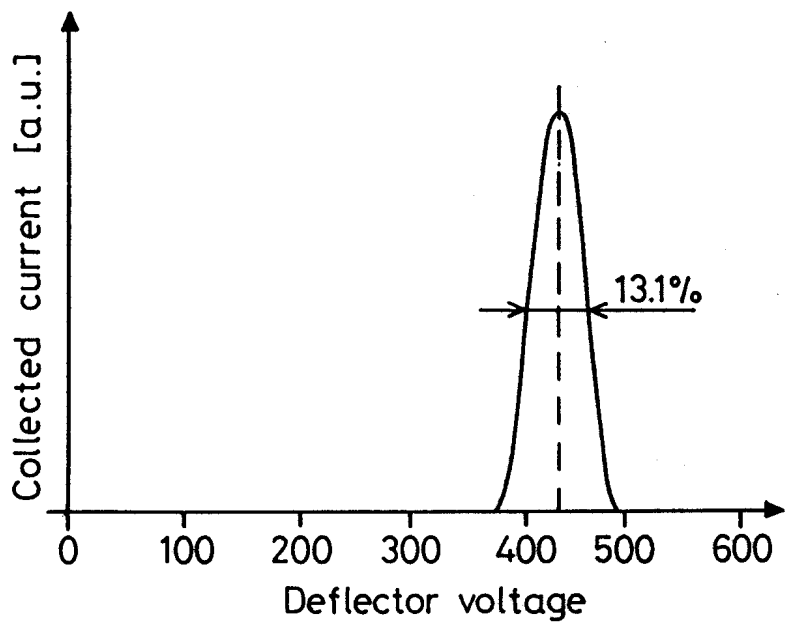


FIG. 2

---

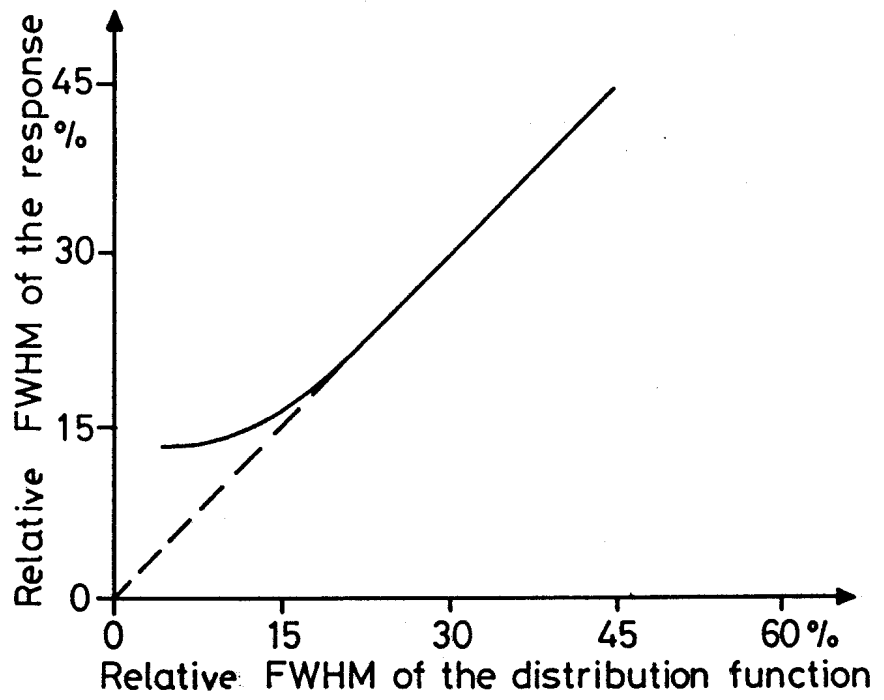


FIG. 3

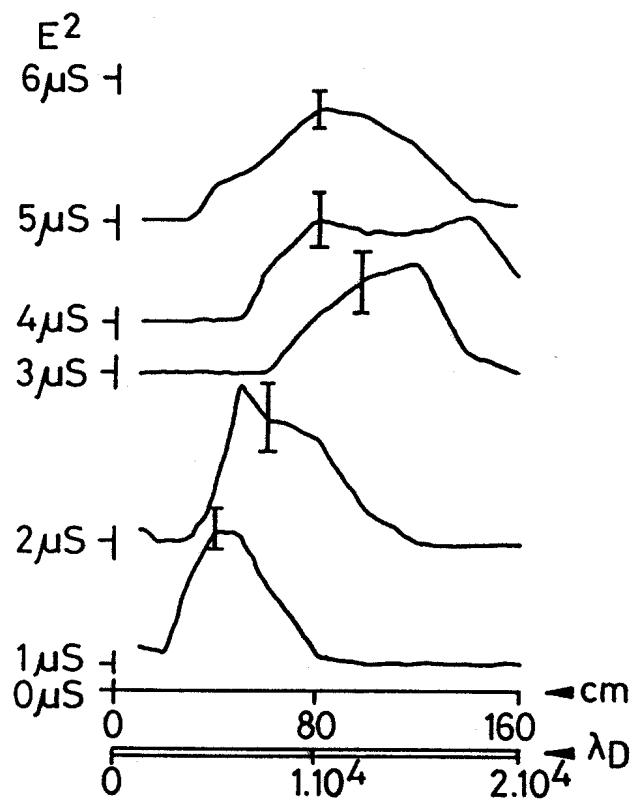


FIG. 4

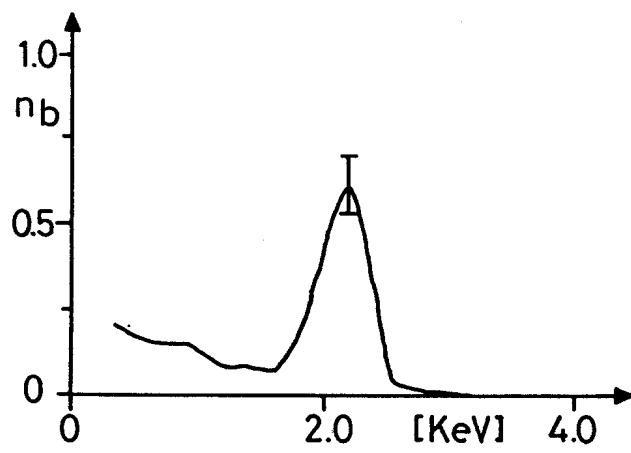


FIG. 5

---



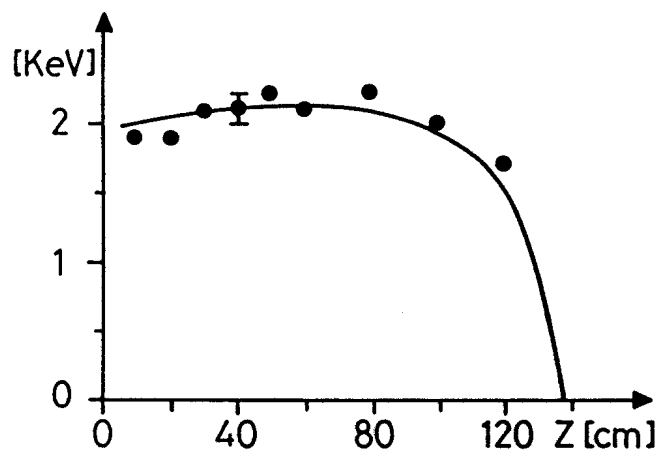


FIG. 6

---

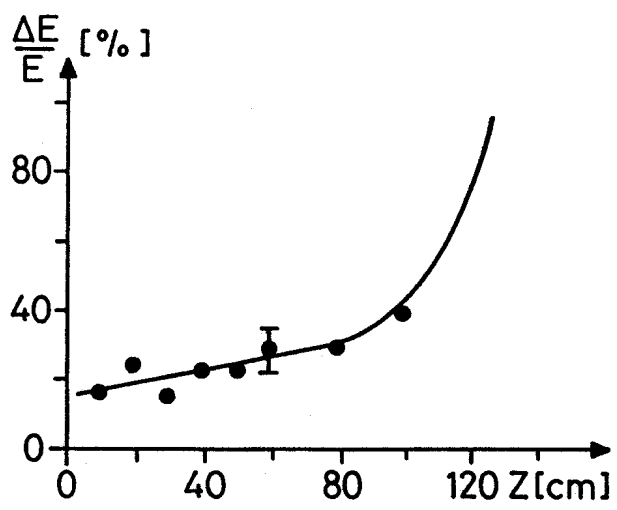


FIG. 7